remote sensing

MDPI

Article

Extreme Change Events of Stratospheric HCl and N_2O in the Mid-Latitude Region of the Northern Hemisphere

Yuanyuan Han [1], Fei Xie [2,*], Fei Cui [3], Feiyang Wang [4], Xin Li [1] and Wuhu Feng [5,6]

[1] Key Laboratory of Textile Chemical Engineering Auxiliaries, School of Environmental and Chemical Engineering, Xi'an Polytechnic University, Xi'an 710048, China
[2] School of Systems Science, Beijing Normal University, Beijing 100875, China
[3] Innovation & Research Institute of HIWING Technology Academy, Beijing 100074, China
[4] College of Oceanography, Hohai University, Nanjing 210098, China
[5] National Centre for Atmospheric Science (NCAS), University of Leeds, Leeds LS2 9JT, UK
[6] Institute for Climate and Atmospheric Science, School of Earth and Environment, University of Leeds, Leeds LS2 9JT, UK
* Correspondence: xiefei@bnu.edu.cn

Abstract: Hydrogen chloride (HCl) is the main reservoir species of chlorine and chemical decomposition of nitrous oxide (N_2O) is the primary source of NO_x (=NO + NO_2) in the stratosphere. Changes in stratospheric HCl and N_2O play a critical role in modulating variations in stratospheric ozone. Thus, long-term trends in stratospheric HCl and N_2O have been investigated in many studies, whereas short-term changes have not received enough attention. Here, using satellite observations and a chemical transport model, we found that two extreme change events for HCl and N_2O in the Northern Hemisphere mid-latitude middle and lower stratosphere have occurred over past decades, which are characterized by a sharp increase in HCl and a decrease in N_2O over several months; for example, HCl increased (and N_2O decreased) by 0.135 ppbv (−33.352 ppbv) in 1987/1988 and by 0.196 ppbv (−28.553 ppbv) in 2010/2011. Further analysis shows that the extreme change events of stratospheric HCl and N_2O in these two periods are closely related to anomalous residual circulation caused by the joint effects of the strong easterly phase of the semi-annual oscillation and the strong polar vortex.

Keywords: stratospheric hydrogen chloride; nitrous oxide; extreme change events; residual circulation; semi-annual oscillation; polar vortex

Citation: Han, Y.; Xie, F.; Cui, F.; Wang, F.; Li, X.; Feng, W. Extreme Change Events of Stratospheric HCl and N_2O in the Mid-Latitude Region of the Northern Hemisphere. *Remote Sens.* **2022**, *14*, 6114. https://doi.org/10.3390/rs14236114

Academic Editor: Carmine Serio

Received: 17 October 2022
Accepted: 30 November 2022
Published: 2 December 2022

1. Introduction

Stratospheric ozone absorbs solar ultraviolet radiation [1–3], protecting life on Earth's surface from biological damage, and via radiative heating, it influences stratospheric temperature and circulation and thus affects global climate change [4–15]. Stratospheric ozone levels began dropping from the late 1970s [16], which was mainly a result of human use of compounds called chlorofluorocarbons (CFCs; [17]). Until 1987, with the implementation of the Montreal Protocol, loading of CFCs in the stratosphere has been reducing, and consequently ozone is projected to recover to pre-1980 levels by the middle of the 21st century [17–20]. However, due to the unpredictable increase or redistribution of substances affecting ozone in the future, such as stratospheric hydrogen chloride (HCl) and nitrous oxide (N_2O), there is still great uncertainty around the recovery of the ozone layer [21–23].

HCl, as the largest reservoir of chlorine in the stratosphere, is important to the gas phase chemical reactions of ozone depletion. Consistent with the decline trend in surface chlorine source gases, the negative trend of stratospheric HCl was observed after 1997 [24–26]. On the basis of satellite observation data, Jones et al. [25] found that HCl in the mid-latitude middle to upper stratosphere showed a decline of −5%/decade from 1997 to 2008. Subsequently, Carpenter and Reimann [26] summarized the results associated

with the recent trend of HCl and concluded a mean decline of 0.6 ± 0.1%/year of HCl in the middle and upper stratosphere for the years 1997–2012. However, in recent years, a significant increasing trend in HCl was observed in the lower stratosphere of the Northern Hemisphere (NH), which is contradictory with continuous monotonic reduction of near-surface source gases and has drawn much attention [27–30]. Mahieu et al. [28] first proposed that there is an increasing trend of HCl in the NH since 2005, which resulted from a weakening of atmospheric circulation.

As the primary source of stratospheric nitrogen oxides (NO_x = NO + NO_2), which are also known to catalyze ozone depletion [31–33], N_2O is expected to remain as the largest emission substance in the stratosphere throughout the 21st century, making it the single most important ozone-depleting emission substance [21,22]. Crutzen and Ehhalt [34] first found the increase in the use of fixed nitrogen as a fertilizer may lead to the reduction of the Earth's ozone layer by several percent at the beginning of the 21st century. Under the IPCC A2 scenario, Portmann and Solomon [35] pointed out that an increase in N_2O may result in a 2–4% reduction of the total ozone column. Using a coupled chemistry–climate model, Wang et al. [36] indicated that a 50%/100% increase in N_2O between 2001 and 2050 will lead to a 6%/10% decrease in ozone mixing ratios in the middle stratosphere at around 10 hPa.

There are several studies reporting that the ozone in the NH has a decreasing trend after the 2000s, e.g., the negative trend of ozone observed in the midlatitudes lower stratosphere [37–40] and Arctic lower stratosphere [41]. This may be closely related with an increasing trend of HCl and N_2O in the NH stratosphere after the 2000s mentioned above. Therefore, trends in stratospheric HCl and N_2O are still of great concern, and thus long-term trends in stratospheric HCl and N_2O have received much attention [24–26,42–46]. In contrast, short-term changes in stratospheric HCl and N_2O in the mid-latitude region of NH have not received as much attention relative to their trends. However, if extreme variations in stratospheric HCl and N_2O in the mid-latitude region of NH do occur, these could create influences on ozone that cannot be ignored. This study defines the extreme change events for stratospheric HCl and N_2O in the mid-latitude region of NH that have occurred in the past few decades and explains the relevant physical mechanisms. The structure of the paper is as follows: Section 2 provides a brief description of the data and methods used; Section 3 presents the analysis of the extreme change events and the relevant physical mechanisms; and conclusions and a discussion are provided in Section 4.

2. Data and Methods

The primary stratospheric HCl and N_2O dataset used was from version 5 of the Aura Microwave Limb Sounder (MLS) level 2 data (https://acdisc.gesdisc.eosdis.nasa.gov/data/Aura_MLS_Level2/, accessed on 1 January 2021), covering the period from 2005 to 2020. MLS measures atmospheric chemical species daily, with a global coverage from 82°N to 82°S and a vertical resolution of ≈3 km for HCl and ≈5–8 km for N_2O [47]. We used the gridded MLS data at a resolution of 4° longitude × 4° latitude; the quality screening rules for this dataset have been previously described by Livesey et al. [47]. For the three-dimensional (3D) winds, temperature, and potential vorticity fields, ERA5 re-analysis datasets from the European Centre for Medium-Range Weather Forecasts (ECMWF, https://www.ecmwf.int/en/forecasts/datasets/reanalysis-datasets/era5, accessed on 1 January 2021) for 1979–2020 were used, with a horizontal resolution of 1° longitude × 1° latitude.

To obtain the long-term changes in stratospheric HCl and N_2O, we used a three-dimensional off-line chemical transport model (TOMCAT/SLIMCAT) [48]. This model uses horizontal winds and temperatures from the fifth major global re-analysis produced by ERA5 [49] and uses a hybrid sigma–pressure vertical coordinate with detailed tropospheric and stratospheric chemistry [50]. Vertical advection is calculated from the divergence of the horizontal mass flux [48], and chemical tracers are advected, conserving second-order moments [51]. The model has been extensively evaluated against various ozone satellite and sounding datasets, providing a good representation of stratospheric chemistry (see, for

example, Chipperfield [48]; Feng et al. [52]; Dhomse et al. [53]). The TOMCAT/SLIMCAT model used for long-term simulation in this study performs with a horizontal resolution of about 2.8° latitude × 2.8° longitude and with 32 levels, from the surface to 65 km altitude.

The latitudinal average zonal wind in the tropical region (10°N–10°S) at 50 hPa is defined as the quasi-biennial oscillation (QBO) index [54]. The semi-annual oscillation (SAO) index is defined as the zonal-mean wind averaged between 10°N–10°S and 1–5 hPa [55]. The polar vortex (PV) intensity is defined using the 10 hPa zonal mean-zonal wind at 60°N [56]. In addition, the transformed Eulerian mean residual circulation ($\overline{v}^*, \overline{w}^*$) was used to diagnose the residual circulation [57]. In pressure coordinates, these are defined by $\overline{v}^* = \overline{v} - \frac{1}{\rho_0}\left(\frac{\rho_0 \overline{v'\theta'}}{\overline{\theta}_z}\right)_z$ and $\overline{w}^* = \overline{w} + \frac{1}{a\cos\varphi}\left(\frac{\cos\varphi \overline{v'\theta'}}{\overline{\theta}_z}\right)_\varphi$. Here, overbars denote zonal means, and primes are deviations from the zonal mean of a given variable; z is log-pressure height and φ is the latitude; v and w are the meridional and vertical velocity, respectively; ρ_0 is density, which is defined as $\rho_0 = \rho_s \exp(-z/H)$ with H = 7.0 km; θ is the potential temperature; and a is the Earth's radius.

3. Results

Figure 1a,b shows the time series for HCl and N_2O anomalies in the NH mid-latitude middle and lower stratosphere from 2005 to 2020 based on MLS data (red line), and from 1979 to 2020 based on the TOMCAT/SLIMCAT simulation (black line). The TOMCAT/SLIMCAT model was employed to reproduce the long-term changes in HCl and N_2O in the stratosphere. It is evident that the changes in stratospheric HCl and N_2O from 2005 to 2020 derived from the TOMCAT/SLIMCAT simulation (black line) are in overall agreement with those from the MLS satellite measurements (red line), providing confidence in the ability of the TOMCAT/SLIMCAT model to reproduce long-term changes in HCl and N_2O in the stratosphere. Here, an extreme change event for stratospheric HCl (N_2O) is defined by two indicators (Figure 1c,d): first, the increase (decrease) magnitude of one event of HCl (N_2O), which is calculated using the maximum value of HCl (minimum value of N_2O) in a year minus the minimum (maximum) value in the past 12 months; second, the increase (decrease) gradient in HCl (N_2O) exceeded the 95th percentile threshold for the whole period, following extreme precipitation events [58]. Note that since the cycle of HCl and N_2O was about 20 months (Figure 2a,b), the difference of extreme value within 12 months was selected to calculate the magnitude changes, and the result was not sensitive to the selected number of months (10 months or 24 months, Figure 2c–f). According to this definition, we found two extreme change events occurred in 1988 and 2011 (Figure 1), with a sharp increase (decrease) of HCl (N_2O) by 0.135 ppbv (−33.352 ppbv) in 1988 and by 0.196 ppbv (−28.553) ppbv in 2011, respectively. Evidently, the anomalies in HCl (N_2O) in 1988 and 2011 are significantly greater than those in other years (Figure 1a,b).

Further analysis showed that both the extreme change events, in 1987/1988 and in 2010/2011, occurred from November to February (Figure 3a,b); therefore, these four months were the main focus of our investigation, as described in the following paragraphs. Compared to N_2O in the troposphere, N_2O in the stratosphere has a much shorter lifetime, but such extreme changes in N_2O within a few months (Figure 1b) should mainly be caused by dynamic transport in the stratosphere [59–61]. The residual circulation in the stratosphere transports trace gases from the tropics to polar regions and thus influences the distribution of trace gases in the stratosphere [62–67]. Dynamic transport associated with residual circulation was considered in order to examine the cause of these extreme change events for stratospheric HCl and N_2O. There are evident downwelling anomalies of the residual circulation in the mid-latitude upper stratosphere from December to February (Figure 3c–f), and upwelling anomalies in the high-latitude middle and lower stratosphere from January to February (Figure 3e,f), in 1987/1988 and 2010/2011. The downwelling anomalies in 1987/1988 and 2010/2011 were greater than those in other years (Figure 3g), and the upwelling anomalies in 1987/1988 and 2010/2011 were also larger than those in most other years (Figure 3h). Note that the stratospheric residual circulation can be divided into the deep branch in the middle to upper stratosphere and the shallow branch in the middle

to lower stratosphere [65,68]. Then, downwelling anomalies of the residual circulation in the mid-latitude upper stratosphere imply an enhancement of the deep branch of the residual circulation in mid-latitude, and upwelling anomalies in the high-latitude middle and lower stratosphere imply a slowdown of the shallow branch of the residual circulation in high latitude compared with the climatology of the residual circulation. Considering that the vertical and meridional gradients of HCl and N_2O distribution are opposite to each other, on the one hand, strengthening of the deep branch of the residual circulation in the mid-latitudes leads to more HCl-rich and N_2O-poor air being transported from the upper stratosphere to the middle and lower stratosphere, resulting in the increase in HCl and decrease in N_2O observed in 1987/1988 and 2010/2011. On the other hand, the weakened shallow branch of the residual circulation in high latitudes weakened the exchange of air between mid-latitudes and high-latitudes. Both of these processes contributed to the sharp increase in HCl and decrease in N_2O in the mid-latitude middle and lower stratosphere in 1987/1988 and 2010/2011.

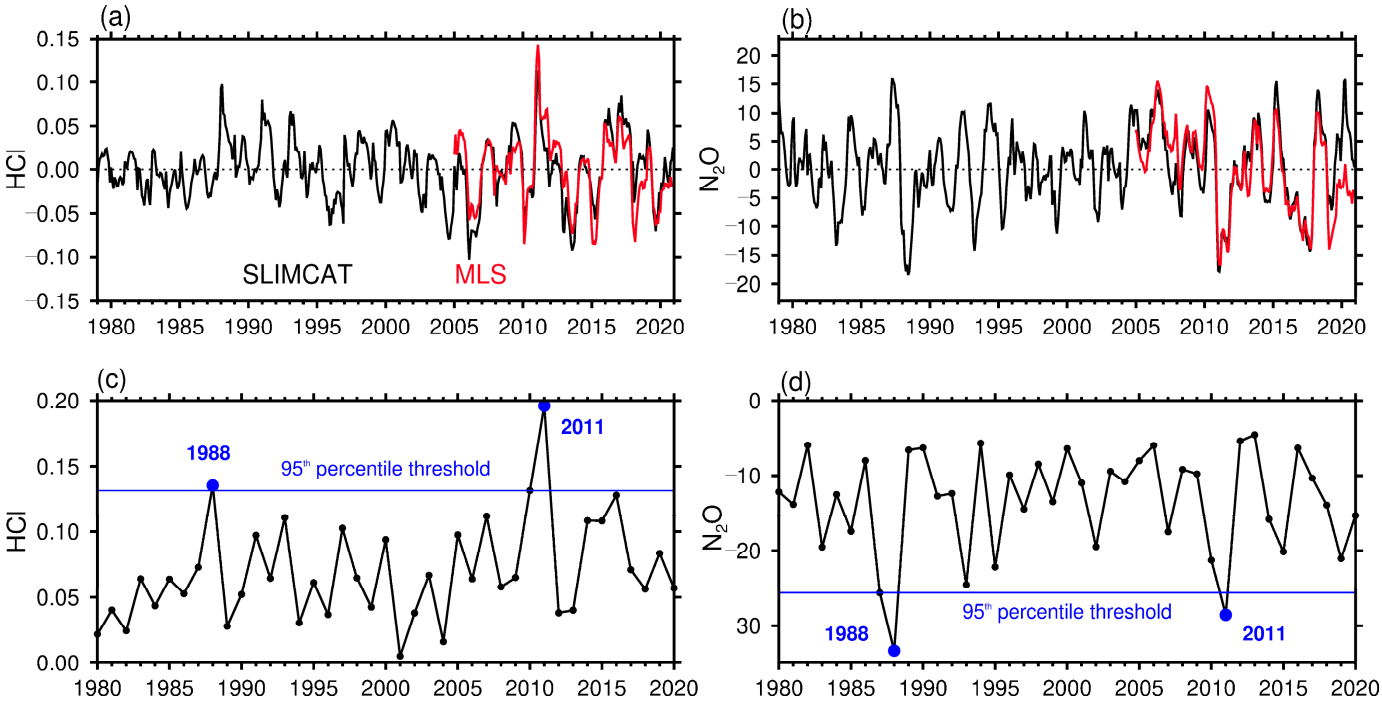

Figure 1. (**a**,**b**) Variation in (**a**) HCl and (**b**) N_2O anomalies in the NH mid-latitude middle and lower stratosphere (20–50°N, 10–50 hPa) from 2005 to 2020 based on MLS data (red line). The linear trends of HCl and N_2O were removed. The black line is based on the SLIMCAT model simulation for the period of 1979 to 2020, and the trend for HCl was removed by splitting the time period (1979–1997, 1997–2021), due to the effectiveness of the Montreal Protocol. (**c**,**d**) Variation in (**c**) HCl and (**d**) N_2O gradient from 1980 to 2020 based on SLIMCAT model simulation. The HCl (N_2O) gradient was calculated using the maximum value of HCl (minimum value of N_2O) in a year minus the minimum (maximum) value in the past 12 months. The blue dots represent the years 1988 and 2011.

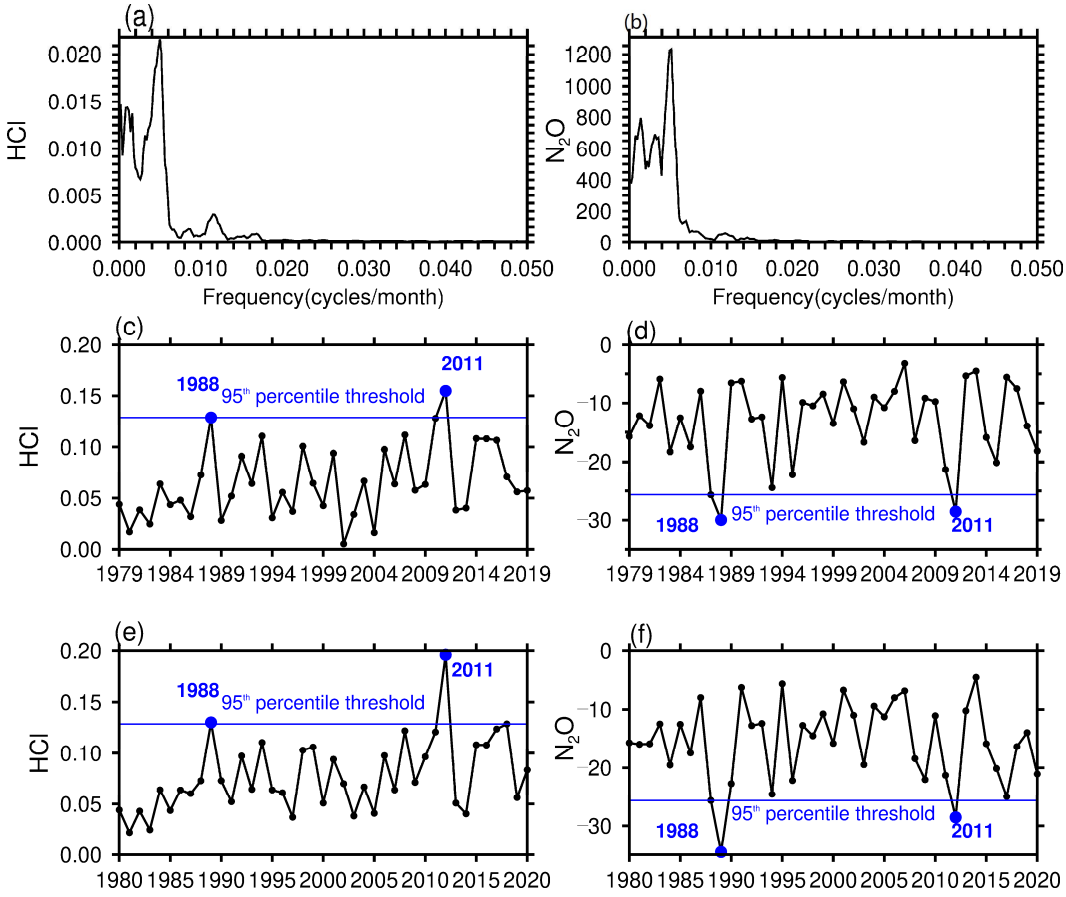

Figure 2. (**a**,**b**) The spectrum of (**a**) HCl and (**b**) N_2O anomalies from 1979 to 2020 based on the SLIMCAT model simulation. (**c**–**f**) Variations in (**c**,**e**) HCl and (**d**,**f**) N_2O gradient based on the SLIMCAT model simulation. The HCl (N_2O) gradient was calculated using the maximum value of HCl (minimum value of N_2O) in a year minus the minimum (maximum) value in the past (**c**,**d**) 10 months and (**e**,**f**) 24 months. The blue dots represent the years 1988 and 2011.

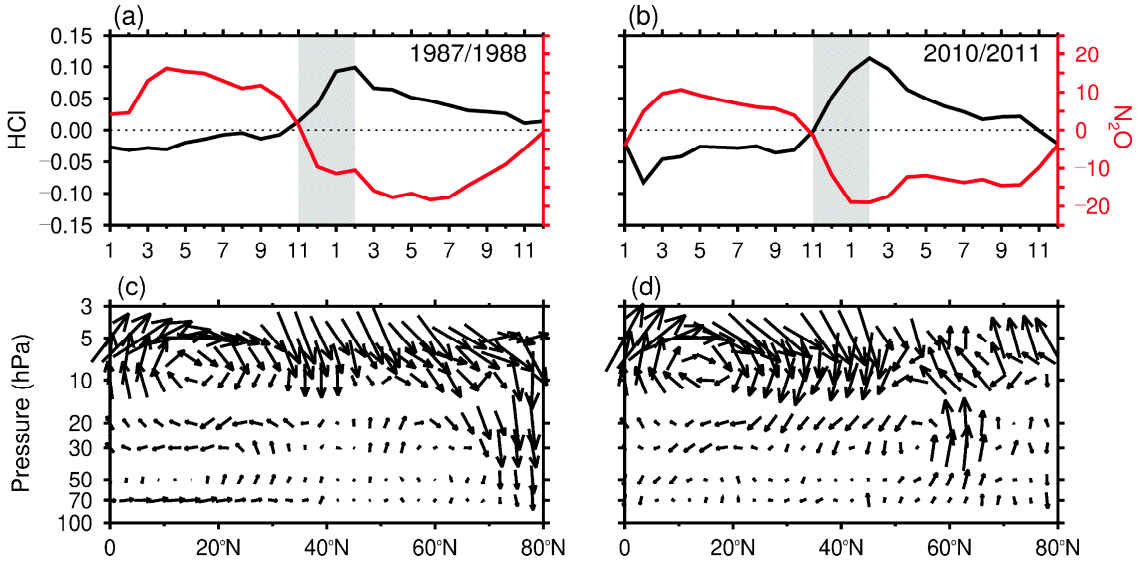

Figure 3. *Cont.*

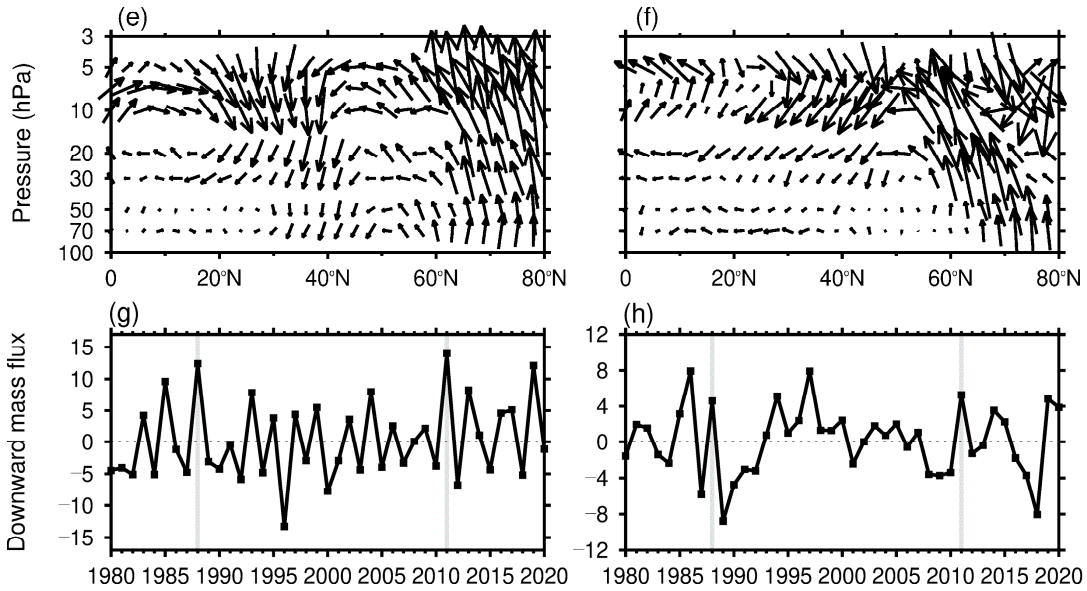

Figure 3. (**a**,**b**) Variation in HCl (black line) and N_2O (red line) from (**a**) January 1987 to December 1988 and (**b**) January 2010 to December 2011 based on the SLIMCAT model simulation. (**c**–**f**) Latitude–height cross-sections of the residual circulation anomaly averaged in (**c**) November–December 1987 and (**d**) November–December 2010; (**e**) January–February 1988 and (**f**) January–February 2011. The vertical component of the residual circulation was multiplied by 500. (**g**,**h**) Variations of (**g**) downward mass flux anomalies in the mid-latitude upper stratosphere (5–10 hPa, 20–50°N) averaged for November–February and (**h**) upward mass flux anomalies in the high-latitude lower stratosphere (20–50 hPa, 65–75°N) averaged for January–February from 1980 to 2020.

To further verify the effect of the residual circulation on the extreme change events of stratospheric HCl and N_2O, Figures 4 and 5 show the month-to-month evolution of HCl + residual circulation anomalies and N_2O + residual circulation anomalies, respectively, from November 2010 to April 2011. Since the changes in stratospheric HCl and N_2O and the relevant residual circulation in 1987/1988 were similar to those in 2010/2011 (Figures 1 and 3), and observations were available for 2010/2011, the case for 2010/2011 is mainly examined here. From November 2010 to February 2011 (Figures 4a–d and 5a–d), there was an evident clockwise cell in the low–mid-latitude middle and upper stratosphere (arrows), accompanied by the strong sinking motion in the mid-latitude upper stratosphere. This implies an enhancement of the deep branch of the residual circulation in the mid-latitude upper stratosphere. The strong downwelling branch leads to HCl-rich and N_2O-poor air being transported from the upper stratosphere to the lower and middle stratosphere, corresponding to an increase in HCl (contours in Figure 4) and decrease in N_2O (contours in Figure 5) just below the position of the strengthening deep branch of the residual circulation. From January 2011 to March 2011 (Figures 4c–e and 5c–e), upwelling anomalies of the residual circulation were found in the high-latitude middle and lower stratosphere, implying a weakened shallow branch of the residual circulation (in Figures 4c–e and 5c–e). Weakened residual circulation slowed down the exchange of air between low–mid latitudes and high latitudes, leading to an accumulation of HCl-rich and N_2O-poor air in the low–mid latitudes (contours in Figures 4c–e and 5c–e). In addition, in the high-latitude middle and lower stratosphere, weakened residual circulation was favorable for chemical decomposition of HCl and N_2O, which is consistent with the evident decrease in HCl and N_2O in high latitudes of the middle and lower stratosphere from January 2011 to March 2011 (contours Figures 4c–e and 5c–e). By April 2011, upwelling anomalies of the residual circulation were small (arrows in Figures 4f and 5f), speeding up the exchange of air between low–mid latitudes and high latitudes. This explains why the center of positive HCl and negative N_2O anomalies moved to high latitudes of the lower stratosphere (contours

in Figures 4f and 5f). The case for 1987/1988 (not shown) agrees with that for 2010/2011 (Figures 4 and 5).

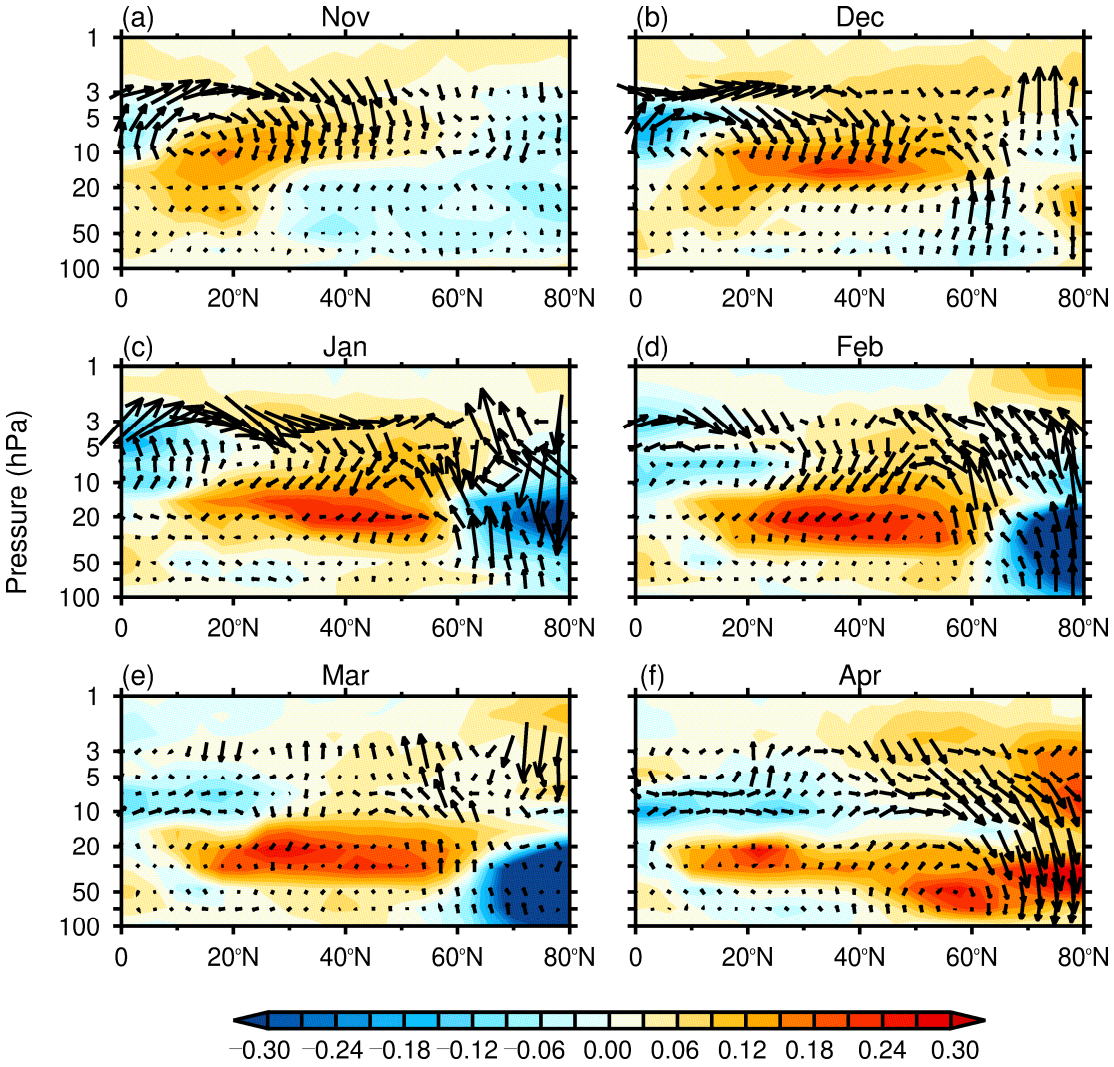

Figure 4. Month-to-month evolution of anomalies of the residual circulation (v^*, w^*, arrows) and HCl (contours) (**a**–**f**) from November 2010 to April 2011. The vertical component of the residual circulation was multiplied by 500. HCl values are based on MLS data.

The reasons for the strengthening deep branch of the residual circulation in mid-latitudes, as well as the weakening shallow branch of the residual circulation in high latitudes in 1987/1988 and 2010/2011, require further investigation. The tropical QBO, the SAO, and the PV are the dominant factors influencing short-term changes of circulation in the upper stratosphere and high latitudes [69–72]. Figure 6 shows QBO, SAO, and PV indices from 1980 to 2020 (see Section 2 for definitions of QBO, SAO, and PV indices). There were strong negative SAO indices and positive PV indices in 1987/1988 and 2010/2011, but the QBO was not in a strong phase. This indicates the simultaneous occurrence of a strong easterly phase of the SAO (ESAO) and a strong polar vortex (SPV). Under the ESAO, clockwise circulation was observed in the NH upper stratosphere (Figure 3c–f), which is consistent with previous studies [55,73]. The circulation induced intense downward transport in the mid-latitude upper stratosphere, coinciding with the location of an enhanced deep branch of the residual circulation. In addition, the SPV corresponded to the weakened wave activity in the NH high-latitude lower stratosphere, which was further consistent with a weakened shallow branch of the residual circulation in NH high latitudes.

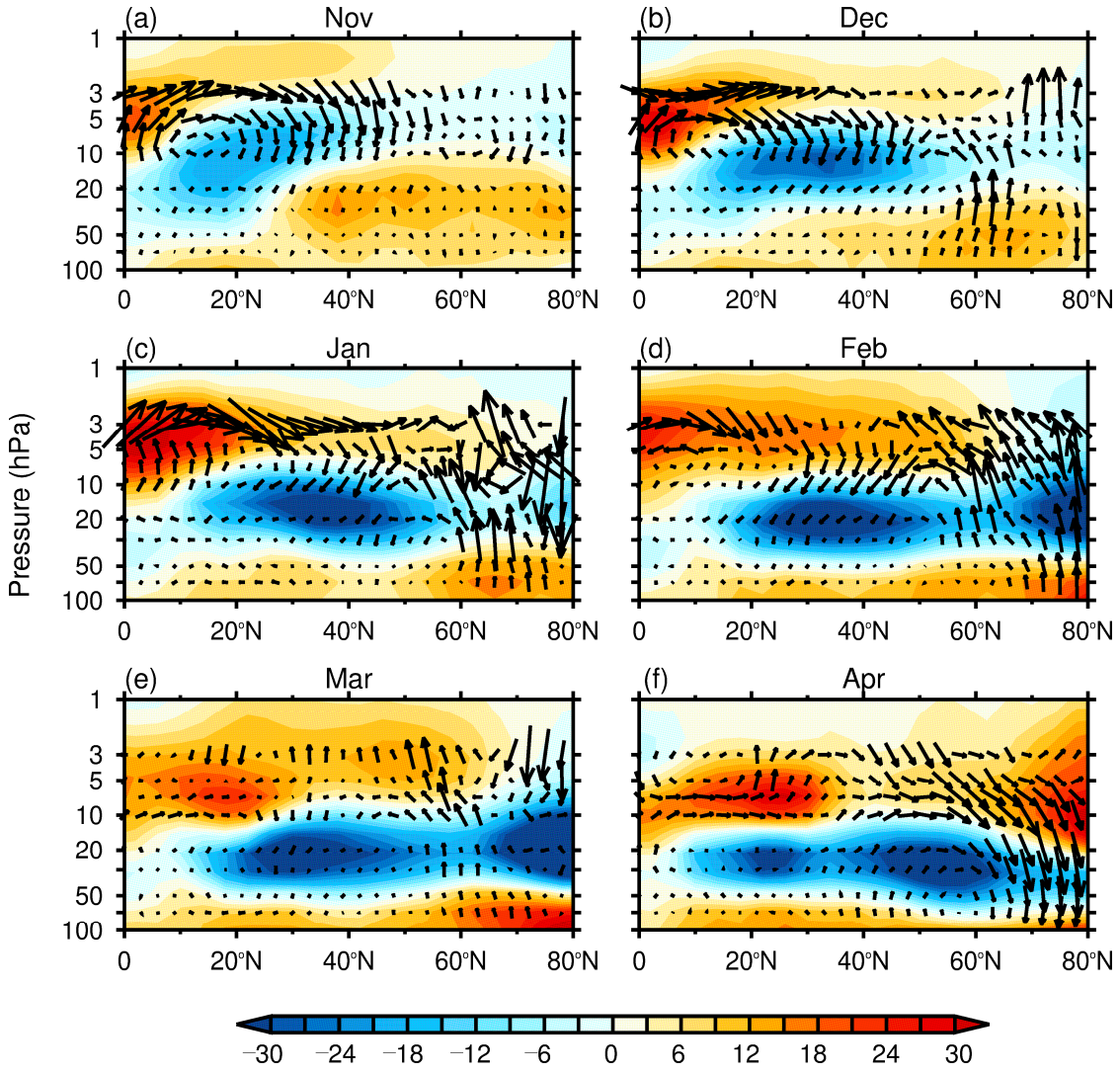

Figure 5. Month-to-month evolution of anomalies of the residual circulation (v^*, w^*, arrows) and N_2O (contours) (**a**–**f**) from November 2010 to April 2011. The vertical component of the residual circulation was multiplied by 500. N_2O values are based on MLS data.

The main characteristic of the meridional circulation associated with the SAO is the existence of tropical areas of convergence and divergence, which are produced by a negative and positive anomaly in the meridional wind in the NH tropical zone [55,74]. To confirm the effect of the SAO on the strengthening deep branch of the residual circulation, month-to-month evolution of the meridional wind anomalies from November 2010 to April 2011 are shown in Figure 7. From November 2010 to February 2011, significant positive meridional wind anomalies were found in the NH tropical upper stratosphere, and negative meridional wind anomalies were found in the NH tropical lower stratosphere (Figure 7a–d), corresponding to the convergence and divergence zones, respectively. The existence of these convergence and divergence zones corresponded to the rising and sinking motions. The rising motion over the tropical wind shear zones and sinking motions over the subtropics and mid-latitudes, added to the meridional divergence and convergence motions, formed a clockwise circulation cell (vectors in Figures 4a–d and 5a–d). Until March 2011, the positive meridional wind anomalies in the tropical upper stratosphere became weak; thus, the corresponding clockwise circulation cell disappeared (Figures 4e, 5e and 7e).

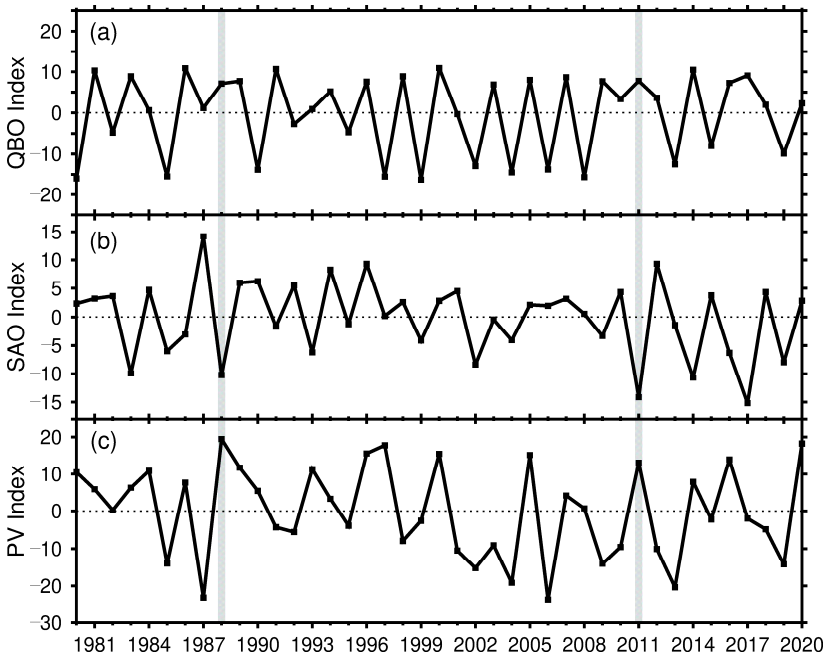

Figure 6. (**a**) QBO and (**b**) SAO indices averaged from November to February and (**c**) PV index averaged in January–February from 1980 to 2020 based on the ERA5 re-analysis dataset.

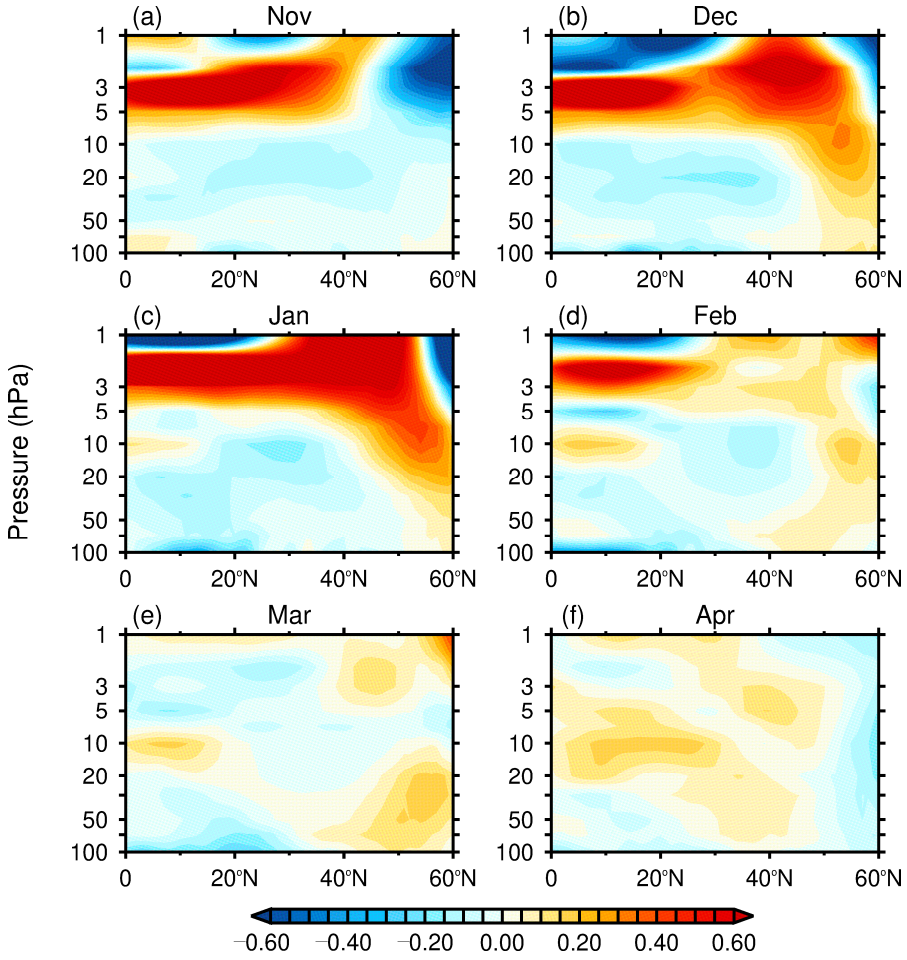

Figure 7. Month-to-month evolution of the meridional wind anomalies (**a**–**f**) from November 2010 to April 2011. Anomalies are defined as the deviations of meridional wind from its seasonal cycle.

Figure 8 further shows the month-to-month evolution of the zonal-mean wind anomalies from November 2010 to April 2011, in order to confirm the effect of a SPV on the weakened shallow branch of the residual circulation. Positive zonal-mean wind anomalies from January 2010 to March 2011 imply an anomalous SPV (Figure 8c–e), corresponding to the weakened residual circulation (Figure 4c–e). In April 2011, the negative zonal-mean wind anomalies in the high latitudes imply the collapse of the polar vortex (Figure 8f), and the corresponding weakened residual circulation disappeared (Figure 4f).

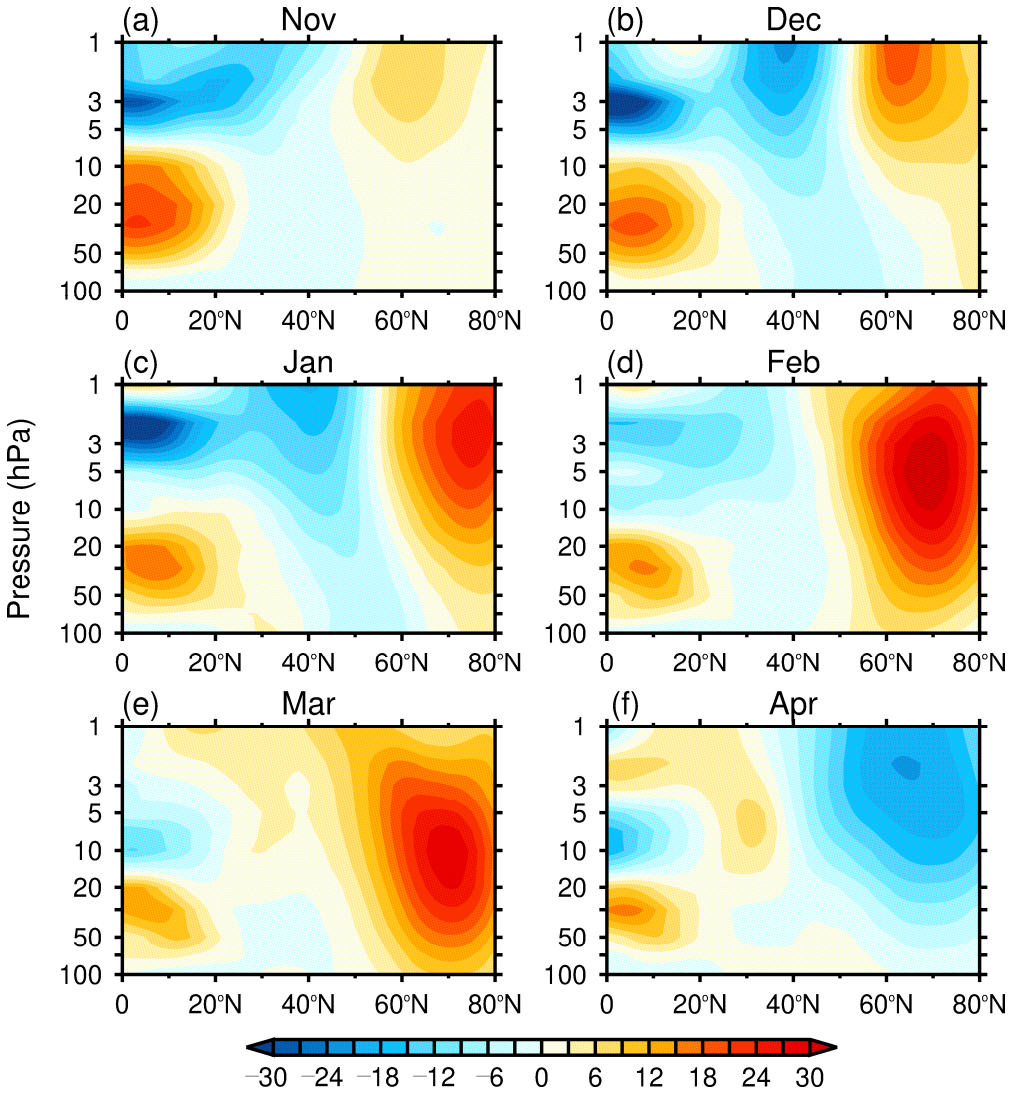

Figure 8. Month-to-month evolution of zonal-mean wind anomalies (**a**–**f**) from November 2010 to April 2011. Anomalies are defined as the deviations of zonal-mean wind from its seasonal cycle.

The above analysis points out the effect of significant anomalous residual circulation on the extreme change events for stratospheric HCl and N_2O in 1987/1988 and 2010/2011, and furthermore indicates that the anomalous residual circulation resulted from the joint effects of ESAO and a SPV. Table 1 shows the simultaneous occurrence of ESAO and SPV from 1979 to 2020 according to the data in Figure 6. It can be seen that the ESAO and SPV only occurred simultaneously in 1987/1988 and 2010/2011. This may explain why the extreme change events for stratospheric HCl and N_2O only occurred in 1987/1988 and 2010/2011.

Table 1. Simultaneous occurrence of the easterly phase of the SAO (ESAO) and the strong polar vortex (SPV) from 1979 to 2020.

Year	ESAO	SPV	Year	ESAO	SPV
1979–1980			2000–2001		
1980–1981			2001–2002		
1981–1982			2002–2003		
1982–1983			2003–2004		
1983–1984			2004–2005		
1984–1985			2005–2006		
1985–1986			2006–2007		
1986–1987			2007–2008		
1987–1988	✓	✓	2008–2009		
1988–1989			2009–2010		
1989–1990			2010–2011	✓	✓
1990–1991			2011–2012		
1991–1992			2012–2013		
1992–1993			2013–2014		
1993–1994			2014–2015		
1994–1995			2015–2016		
1995–1996			2016–2017		
1996–1997			2017–2018		
1997–1998			2018–2019		
1998–1999			2019–2020		
1999–2000					

SAO index lower than a negative standard deviation and PV index larger than a positive standard deviation were selected as the ESAO and SPV events, respectively.

4. Conclusions and Discussion

In this paper, we investigated extreme change events of stratospheric HCl and N_2O concentrations in the mid-latitude region of the NH middle and lower stratosphere by using the latest satellite observations and a chemical transport model. From 1979 to 2020, there were two extreme change events of stratospheric HCl and N_2O in the NH middle and lower stratosphere, one in 1987/1988 and one in 2010/2011, which were characterized by a sharp increase in HCl and decrease in N_2O over several months. These extreme change events were closely related to significant anomalous residual circulation; that is, a stronger deep branch of the residual circulation in the mid-latitude upper stratosphere brought about more HCl-rich and N_2O-poor air from the upper stratosphere down to the lower stratosphere; meanwhile, a slowdown of the shallow branch of the residual circulation in the high-latitude middle and lower stratosphere weakened the transport of air between mid-latitudes and high latitudes. Both of these processes contributed to the sharp increase in HCl and a decrease in N_2O recorded in the mid-latitude lower stratosphere in 1987/1988 and in 2010/2011. Further analysis suggests that during the period from 1979 to 2020, strong ESAO and SPV occurred simultaneously in 1987/1988 and 2010/2011 and were responsible for the significant anomalous residual circulation.

The question arises here as to whether the westerly phase of the SAO (WSAO) and a weakened polar vortex (WPV) would induce the opposite effect on stratospheric HCl and N_2O changes. The simultaneous occurrence of the WSAO and WPV from 1979 to 2020 is also presented in Table 2. It was found that only in 1986/1987 did the WSAO and WPV occur simultaneously, corresponding to a decrease in HCl and an increase in N_2O (Figure 9a), but the magnitude of the change was smaller than those observed in 1987/1988 and 2010/2011 (Figure 3a,b) and not evident from the data for the variation in HCl and N_2O (Figure 1). Figure 9b,c further shows the anomalies in the residual circulation in 1986/1987. Under the influence of the WSAO and WPV, anti-clockwise circulation in the low–mid-latitude upper stratosphere and downwelling mass flux anomalies in the high-latitude middle and lower stratosphere were evident (Figure 9b), which is opposite from what was observed in 1987/1988 and 2010/2011 (Figure 3c–f). The strength of the

ascending motion of the anti-clockwise circulation and downwelling mass flux anomalies in 1986/1987 was significantly smaller than that in 1987/1988 and 2010/2011 (Figures 3c–f and 9c), and this may explain why the changes in stratospheric HCl and N_2O caused by the joint effects of the WSAO and WPV (1986/1987) were not evident.

Table 2. Simultaneous occurrence of the westerly phase of the SAO (WSAO) and weakened polar vortex (WPV) in winter from 1979 to 2020.

Year	WSAO	WPV	Year	WSAO	WPV
1979–1980			2000–2001		
1980–1981			2001–2002		
1981–1982			2002–2003		
1982–1983			2003–2004		
1983–1984			2004–2005		
1984–1985			2005–2006		
1985–1986			2006–2007		
1986–1987	✓	✓	2007–2008		
1987–1988			2008–2009		
1988–1989			2009–2010		
1989–1990			2010–2011		
1990–1991			2011–2012		
1991–1992			2012–2013		
1992–1993			2013–2014		
1993–1994			2014–2015		
1994–1995			2015–2016		
1995–1996			2016–2017		
1996–1997			2017–2018		
1997–1998			2018–2019		
1998–1999			2019–2020		
1999–2000					

SAO index larger than a positive standard deviation and NAM index lower than a negative standard deviation were selected as the WSAO and WPV events, respectively.

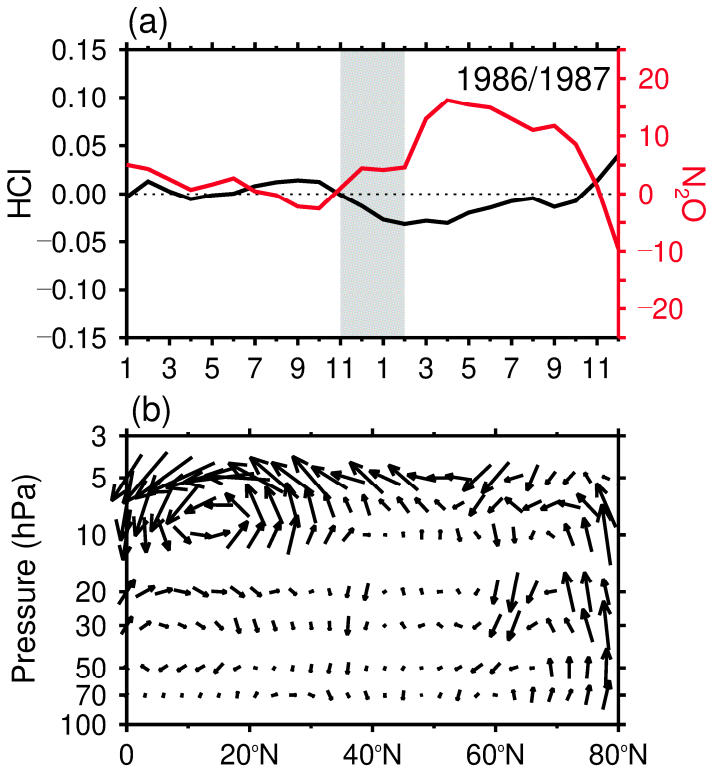

Figure 9. *Cont.*

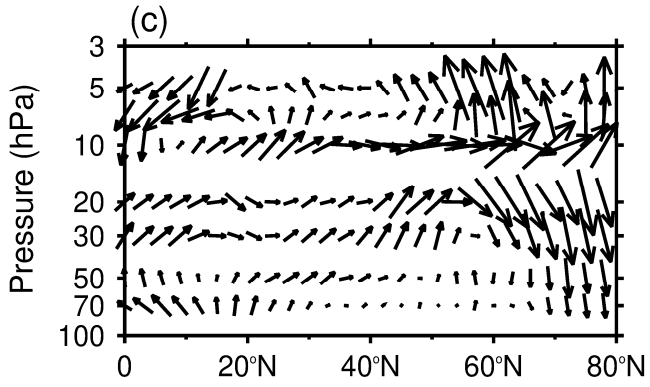

Figure 9. (**a**) Variation in HCl (black line) and N_2O (red line) from January 1986 to December 1987 based on SLIMCAT model simulation. (**b**) Latitude–height cross-sections of the residual circulation anomaly averaged in (**b**) November–December 1986 and (**c**) January–February 1987. The vertical component of the residual circulation was multiplied by 500.

In addition, the extreme change events above mainly represent the extreme decrease in HCl and increase in N_2O, and then whether there were reversed extreme HCl and N_2O events from 1979 to 2020. Figure 10 shows the variations of the HCl (N_2O) gradient that was calculated using the minimum value of HCl (maximum value of N_2O) in a year minus the maximum (minimum) value in the past 12 months. According to the definition of an extreme change event, extreme decease events of HCl were found in 2010 and 2019, and extreme increase events of N_2O were found in 2018 and 2020. Unlike in 1988 and 2011, reversed extreme change events of HCl and N_2O did not occur at the same time. This may be related to the climatology distribution of HCl and N_2O or to the changes of the residual circulation having different effects on the chemical reactions of HCl and N_2O.

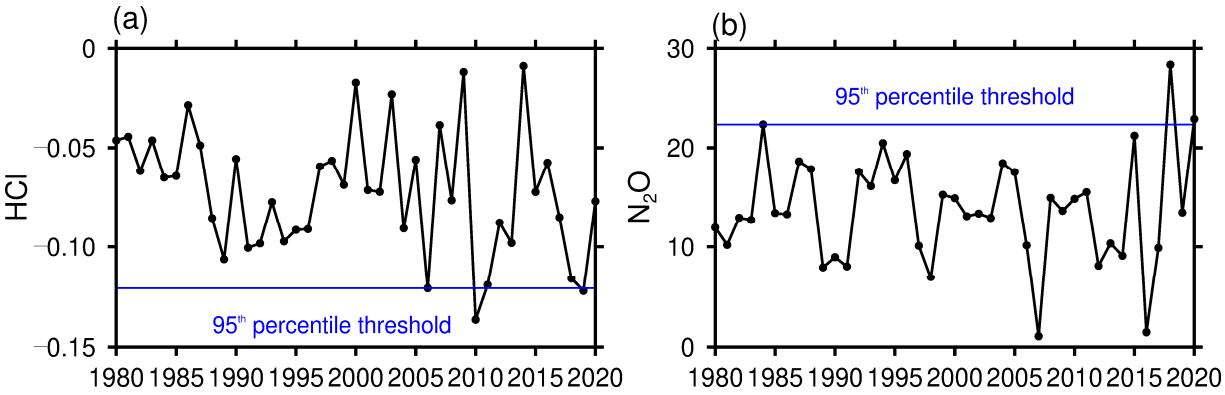

Figure 10. Variations in (**a**) HCl and (**b**) N_2O gradient from 1980 to 2020 based on SLIMCAT model simulation. The HCl (N_2O) gradient was calculated using the minimum value of HCl (maximum value of N_2O) in a year minus the maximum (minimum) value in the past 12 months.

There are still issues worthy of further study with regard to changes in HCl and N_2O. For example, how much impact would these extreme change events for HCl and N_2O have on ozone? Moreover, will there be more and more extreme change events occurring in the future?

Author Contributions: Conceptualization, F.X.; methodology, Y.H. and F.X.; software, Y.H.; validation, Y.H., F.C., and F.W.; formal analysis, Y.H. and X.L.; investigation, Y.H. and F.X.; data curation, Y.H., F.C., W.F., and X.L.; writing—original draft preparation, Y.H. and F.X.; visualization, Y.H., F.C., and F.W.; supervision, Y.H. and F.X.; project administration, F.X.; funding acquisition, Y.H. and F.X.; writing—review and editing, Y.H., F.X., and W.F. All authors have read and agreed to the published version of the manuscript.

Funding: This work was supported by the National Natural Science Foundation of China (42275084, 42122037, 41905039) and the Natural Science Basic Research Program in Shaanxi Province of China (2022JM-142).

Data Availability Statement: The original observational data used in this study are publicly available and can be downloaded from the corresponding websites (MLS dataset: https://acdisc.gesdisc.eosdis.nasa.gov/data/Aura_MLS_Level2/, accessed on 1 January 2021; ERA5 data: https://www.ecmwf.int/en/forecasts/datasets/reanalysis-datasets/era5, accessed on 1 January 2021).

Acknowledgments: We acknowledge meteorological fields from ECWMF ERA5, HCl/N_2O data from the NASA MLS, and TOMCAT/SLIMCAT from the UK National Centre for Atmospheric Science (NCAS).

Conflicts of Interest: The authors declare no conflict of interest.

References

1. Kerr, J.B.; McElroy, C.T. Evidence for large upward trends of ultraviolet-B radiation linked to ozone depletion. *Science* **1993**, *262*, 1032–1034. [CrossRef]
2. Bais, A.F.; Bernhard, G.; McKenzie, R.L.; Aucamp, P.J.; Young, P.J.; Ilyas, M.; Jöckel, P.; Deushi, M. Ozone–climate interactions and effects on solar ultraviolet radiation. *Photochem. Photobiol. Sci.* **2019**, *18*, 602–640. [CrossRef]
3. Lucas, R.M.; Yazar, S.; Young, A.R.; Norval, M.; de Gruijl, F.R.; Takizawa, Y.; Rhodes, L.E.; Sinclair, C.A.; Neale, R. Human health in relation to exposure to solar ultraviolet radiation under changing stratospheric ozone and climate. *Photochem. Photobiol. Sci.* **2019**, *18*, 641–680. [CrossRef]
4. de F. Forster, P.M.; Shine, K.P. Radiative forcing and temperature trends from stratospheric ozone changes. *J. Geophys. Res. Atmos.* **1997**, *102*, 10841–10855.
5. Son, S.-W.; Polvani, L.M.; Waugh, D.W.; Akiyoshi, H.; Garcia, R.; Kinnison, D.; Pawson, S.; Rozanov, E.; Shepherd, T.G.; Shibata, K. The impact of stratospheric ozone recovery on the Southern Hemisphere westerly jet. *Science* **2008**, *320*, 1486–1489. [CrossRef]
6. Son, S.-W.; Polvani, L.M.; Waugh, D.W.; Birner, T.; Akiyoshi, H.; Garcia, R.R.; Gettelman, A.; Plummer, D.A.; Rozanov, E. The impact of stratospheric ozone recovery on tropopause height trends. *J. Clim.* **2009**, *22*, 429–445. [CrossRef]
7. Hu, D.Z.; Tian, W.S.; Xie, F.; Wang, C.X.; Zhang, J.K. Impacts of stratospheric ozone depletion and recovery on wave propagation in the boreal winter stratosphere. *J. Geophys. Res. Atmos.* **2015**, *120*, 8299–8317. [CrossRef]
8. Nowack, P.J.; Abraham, N.L.; Maycock, A.C.; Braesicke, P.; Gregory, J.M.; Joshi, M.J.; Osprey, A.; Pyle, J.A. A large ozone-circulation feedback and its implications for global warming assessments. *Nat. Clim. Chang.* **2015**, *5*, 41–45. [CrossRef]
9. Nowack, P.J.; Abraham, N.L.; Braesicke, P.; Pyle, J.A. The impact of stratospheric ozone feedbacks on climate sensitivity estimates. *J. Geophys. Res. Atmos.* **2018**, *123*, 4630–4641. [CrossRef]
10. Xie, F.; Li, J.P.; Tian, W.S.; Fu, Q.; Jin, F.-F.; Hu, Y.Y.; Zhang, J.K.; Wang, W.K.; Sun, C.; Feng, J. A connection from Arctic stratospheric ozone to El Niño-Southern oscillation. *Environ. Res. Lett.* **2016**, *11*, 124026. [CrossRef]
11. Xie, F.; Li, J.P.; Zhang, J.K.; Tian, W.S.; Hu, Y.Y.; Zhao, S.; Sun, C.; Ding, R.Q.; Feng, J.; Yang, Y. Variations in North Pacific sea surface temperature caused by Arctic stratospheric ozone anomalies. *Environ. Res. Lett.* **2017**, *12*, 114023. [CrossRef]
12. Maleska, S.; Smith, K.L.; Virgin, J. Impacts of stratospheric ozone extremes on Arctic high cloud. *J. Clim.* **2020**, *33*, 8869–8884. [CrossRef]
13. Xia, Y.; Wang, Y.; Huang, Y.; Hu, Y.Y.; Bian, J.C.; Zhao, C.F.; Sun, C. Significant contribution of stratospheric water vapor to the poleward expansion of the Hadley circulation in autumn under greenhouse warming. *Geophys. Res. Lett.* **2021**, *48*, e2021GL094008. [CrossRef]
14. Friedel, M.; Chiodo, G.; Stenke, A.; Domeisen, D.I.; Fueglistaler, S.; Anet, J.G.; Peter, T. Springtime arctic ozone depletion forces northern hemisphere climate anomalies. *Nat. Geosci.* **2022**, *15*, 541–547. [CrossRef]
15. Oh, J.; Son, S.-W.; Choi, J.; Lim, E.-P.; Garfinkel, C.; Hendon, H.; Kim, Y.; Kang, H.-S. Impact of stratospheric ozone on the subseasonal prediction in the southern hemisphere spring. *Prog. Earth Planet. Sc.* **2022**, *9*, 1–9. [CrossRef]
16. Molina, M.J.; Rowland, F.S. Stratospheric sink for chlorofluoromethanes: Chlorine atom-catalysed destruction of ozone. *Nature* **1974**, *249*, 810–812. [CrossRef]
17. Solomon, S.; Ivy, D.J.; Kinnison, D.; Mills, M.J.; Neely, R.R.; Schmidt, A. Emergence of healing in the Antarctic ozone layer. *Science* **2016**, *353*, 269–274. [CrossRef]
18. Weatherhead, E.C.; Andersen, S.B. The search for signs of recovery of the ozone layer. *Nature* **2006**, *441*, 518–522. [CrossRef]
19. WMO. *Scientific Assessment of Ozone Depletion: 2007*; Report No. 50, Global Ozone Research and Monitoring Project; WMO: Geneva, Switzerland, 2007.
20. WMO. *Scientific Assessment of Ozone Depletion: 2010*; Report No. 52, Global Ozone Research and Monitoring Project; WMO: Geneva, Switzerland, 2011; p. 517.
21. Ravishankara, A.R.; Daniel, J.S.; Portmann, R.W. Nitrous Oxide (N_2O): The Dominant Ozone-Depleting Substance Emitted in the 21st Century. *Science* **2009**, *326*, 123–125. [CrossRef]

22. Revell, L.E.; Tummon, F.; Salawitch, R.J.; Stenke, A.; Peter, T. The changing ozone depletion potential of N2O in a future climate. *Geophys. Res. Lett.* **2015**, *42*, 10047–10055. [CrossRef]
23. Zhang, J.K.; Tian, W.S.; Xie, F.; Chipperfield, M.P.; Feng, W.H.; Son, S.-W.; Abraham, N.L.; Archibald, A.T.; Bekki, S.; Butchart, N.; et al. Stratospheric ozone loss over the Eurasian continent induced by the polar vortex shift. *Nat. Commun.* **2018**, *9*, 489. [CrossRef]
24. Froidevaux, L.; Livesey, N.J.; Read, W.G.; Salawitch, R.J.; Waters, J.W.; Drouin, B.; MacKenzie, I.A.; Pumphrey, H.C.; Bernath, P.; Boone, C. Temporal decrease in upper atmospheric chlorine. *Geophys. Res. Lett.* **2006**, *33*, L23812. [CrossRef]
25. Jones, A.; Urban, J.; Murtagh, D.P.; Sanchez, C.; Walker, K.A.; Livesay, L.; Froidevaux, L.; Santee, M. Analysis of HCl and ClO time series in the upper stratosphere using satellite data sets. *Atmos. Chem. Phys.* **2011**, *10*, 5321–5333. [CrossRef]
26. Carpenter, L.J.; Reismann, S.; Burkholder, J.B.; Clerbaux, C.; Hall, B.D.; Hossaini, R.; Laube, J.C.; Yvon-Lewis, S.A. Ozone-Depleting Substances (ODSs) and other gases of interest to the Montreal Protocol. 2014. 1.1-1.101. Available online: https://hal.archives-ouvertes.fr/hal-01130807 (accessed on 1 January 2021).
27. Kohlhepp, R.; Ruhnke, R.; Chipperfield, M.P.; De Mazière, M.; Notholt, J.; Barthlott, S.; Batchelor, R.L.; Blatherwick, R.D.; Blumenstock, T.; Coffey, M.T.; et al. Observed and simulated time evolution of HCl, ClONO2, and HF total column abundances. *Atmos. Chem. Phys.* **2012**, *12*, 3527–3557. [CrossRef]
28. Mahieu, E.; Chipperfield, M.P.; Notholt, J.; Reddmann, T.; Anderson, J.; Bernath, P.F.; Blumenstock, T.; Coffey, M.T.; Dhomse, S.S.; Feng, W.; et al. Recent Northern Hemisphere stratospheric HCl increase due to atmospheric circulation changes. *Nature* **2014**, *515*, 104–107. [CrossRef]
29. Han, Y.Y.; Tian, W.S.; Chipperfield, M.P.; Zhang, J.K.; Wang, F.Y.; Sang, W.J.; Luo, J.L.; Feng, W.H.; Chrysanthou, A.; Tian, H.Y. Attribution of the hemispheric asymmetries in trends of stratospheric trace gases inferred from Microwave Limb Sounder (MLS) measurements. *J. Geophys. Res. Atmos.* **2019**, *124*, 6283–6293. [CrossRef]
30. Han, Y.Y.; Xie, F.; Zhang, J.K. Has Stratospheric HCl in the Northern Hemisphere Been Increasing Since 2005? *Front. Earth Sci.* **2020**, *8*, 609411. [CrossRef]
31. Mount, G.H.; Solomon, S.; Sanders, R.W.; Jakoubek, R.O.; Schmeltekopf, A.L. Observations of Stratospheric NO_2 and O_3 at Thule, Greenland. *Science* **1988**, *242*, 555–558. [CrossRef]
32. Portmann, R.W.; Daniel, J.S.; Ravishankara, A.R. Stratospheric ozone depletion due to nitrous oxide: Influences of other gases. *Philos. Trans. R. Soc. Lond. Ser. B Biol. Sci.* **2012**, *367*, 1256–1264. [CrossRef]
33. Jaffe, D.A.; Ninneman, M.; Chan, H.C. NO_x and O_3 Trends at US Non-Attainment Areas for 1995–2020: Influence of COVID-19 Reductions and Wildland Fires on Policy-Relevant Concentrations. *J. Geophys. Res. Atmos.* **2022**, *127*, e2021JD036385. [CrossRef]
34. Crutzen, P.J.; Ehhalt, D.H. Effects of nitrogen fertilizers and combustion on the stratospheric ozone layer. *Ambio* **1977**, *6*, 112–117.
35. Portmann, R.W.; Solomon, S. Indirect radiative forcing of theozone layer during the 21st century. *Geophys. Res. Lett.* **2007**, *34*, L02813. [CrossRef]
36. Wang, W.K.; Tian, W.S.; Dhomse, S.S.; Xie, F.; Shu, J.C.; Austin, J. Stratospheric ozone depletion from future nitrous oxide increases. *Atmos. Chem. Phys.* **2014**, *14*, 12967–12982. [CrossRef]
37. Wargan, K.; Orbe, C.; Pawson, S.; Ziemke, J.R.; Oman, L.D.; Olsen, M.A.; Coy, L.; Knowland, K.E. Recent decline in extratropical lower stratospheric ozone attributed to circulation changes. *Geophys. Res. Lett.* **2018**, *45*, 5166–5176. [CrossRef] [PubMed]
38. Ball, W.T.; Alsing, J.; Mortlock, D.J.; Staehelin, J.; Haigh, J.D.; Peter, T.; Yummon, F.; Stübi, R.; Stenke, A.; Anderson, J.; et al. Evidence for a continuous decline in lower stratospheric ozone offsetting ozone layer recovery. *Atmos. Chem. Phys.* **2018**, *18*, 1379–1394. [CrossRef]
39. Chipperfield, M.P.; Dhomse, S.; Hossaini, R.; Feng, W.H.; Santee, M.L.; Weber, M.; Burrows, J.P.; Wild, J.D.; Loyola, D.; Coldewey-Egbers, M. On the cause of recent variations in lower stratospheric ozone. *Geophys. Res. Lett.* **2018**, *45*, 5718–5726. [CrossRef]
40. Orbe, C.; Wargan, K.; Pawson, S.; Oman, L.D. Mechanisms linked to recent ozone decreases in the Northern Hemisphere lower stratosphere. *J. Geophys. Res.* **2022**, *125*, e2019JD031631. [CrossRef]
41. Hu, D.Z.; Guan, Z.Y.; Liu, M.C.; Feng, W.H. Dynamical mechanisms for the recent ozone depletion in the Arctic stratosphere linked to North Pacific sea surface temperatures. *Clim. Dyn.* **2022**, *58*, 2663–2679. [CrossRef]
42. McLinden, C.A.; Prather, M.J.; Liley, J.B.; Olsen, S.C. Understanding trends in stratospheric NOy and NO2. *J. Geophys. Res-Biogeo.* **2001**, *106*, 27787–27794. [CrossRef]
43. Park, S.; Croteau, P.; Boering, K.A.; Etheridge, D.M.; Ferretti, D.; Fraser, P.J.; Kim, K.-R.; Krummel, P.B.; Langenfelds, R.L.; Ommen, T.D.V.; et al. Trends and seasonal cycles in the isotopic composition of nitrous oxide since 1940. *Nat. Geosci.* **2012**, *5*, 261–265. [CrossRef]
44. Nedoluha, G.E.; Boyd, I.S.; Parrish, A.; Gomez, R.M.; Allen, D.R.; Froidevaux, L.; Connor, B.J.; Querel, R.R. Unusual stratospheric ozone anomalies observed in 22 years of measurements from Lauder, New Zealand. *Atmos. Chem. Phys.* **2015**, *15*, 7817–7827. [CrossRef]
45. Kracher, D.; Reick, C.H.; Manzini, E.; Schultz, M.G.; Stein, O. Climate change reduces warming potential of nitrous oxide by an enhanced Brewer-Dobson circulation. *Geophys. Res. Lett.* **2016**, *43*, 5851–5859. [CrossRef]
46. Livesey, N.J.; Read, W.G.; Froidevaux, L.; Lambert, A.; Santee, M.L.; Schwartz, M.J.; Millán, L.F.; Jarnot, R.F.; Wagner, P.A.; Hurst, D.F. Investigation and amelioration of long-term instrumental drifts in water vapor and nitrous oxide measurements from the Aura Microwave Limb Sounder (MLS) and their implications for studies of variability and trends. *Atmos. Chem. Phys.* **2021**, *21*, 15409–15430. [CrossRef]

47. Livesey, N.J.; Read, W.G.; Wagner, P.A.; Froidevaux, L.; Santee, M.L.; Schwartz, M.J. *Version 5.0 x Level 2 and 3 Data Quality and Description Document*; Tech. Rep. No. JPL D-105336 Rev. A; Jet Propulsion Laboratory: Pasadena, CA, USA, 2020.
48. Chipperfield, M.P. New version of the TOMCAT/SLIMCAT off-line chemical transport model: Intercomparison of stratospheric tracer experiments. *Q. J. R. Meteorol. Soc.* **2006**, *132*, 1179–1203. [CrossRef]
49. Hersbach, H.; Bell, B.; Berrisford, P.; Hirahara, S.; Horányi, A.; Muñoz-Sabater, J.; Simmons, A. The ERA5 global reanalysis. *Q. J. R. Meteorol. Soc.* **2020**, *146*, 1999–2049. [CrossRef]
50. Feng, W.H.; Dhomse, S.S.; Arosio, C.; Weber, M.; Burrows, J.P.; Santee, M.L.; Chipperfield, M.P. Arctic ozone depletion in 2019/20: Roles of chemistry, dynamics and the Montreal Protocol. *Geophys. Res. Lett.* **2021**, *48*, e2020GL091911. [CrossRef]
51. Prather, M.J. Numerical advection by conservation of second-order moments. *J. Geophys. Res. Atmos.* **1986**, *91*, 6671–6681. [CrossRef]
52. Feng, W.; Chipperfield, M.P.; Davies, S.; Gathen, P.v.d.; Kyrö, E.; Volk, C.M.; Ulanovsky, A.; Belyaev, G. Large chemical ozone loss in 2004/2005 Arctic winter/spring. *Geophys. Res. Lett.* **2007**, *34*, L09803. [CrossRef]
53. Dhomse, S.S.; Chipperfield, M.P.; Feng, W.; Hossaini, R.; Mann, G.W.; Santee, M.L.; Weber, M. A single-peak-structured solar cycle signal in stratospheric ozone based on Microwave Limb Sounder observations and model simulations. *Atmos. Chem. Phys.* **2022**, *22*, 903–916. [CrossRef]
54. Holton, J.R.; Tan, H.-C. The influence of the equatorial quasi-biennial oscillation on the global circulation at 50 mb. *J. Atmos. Sci.* **1980**, *37*, 2200–2208. [CrossRef]
55. Choi, W.; Lee, H.; Grant, W.B.; Park, J.H.; Holton, J.R.; Lee, K.-M.; Naujokat, B. On the secondary meridional circulation associated with the quasi-biennial oscillation. *Tellus B* **2002**, *54*, 395–406. [CrossRef]
56. Charlton, A.J.; Polvani, L.M. A new look at stratospheric sudden warmings. Part I: Climatology and modeling benchmarks. *J. Climate* **2007**, *20*, 449–469. [CrossRef]
57. Andrews, D.G.; Holton, J.R.; Leovy, C.B. *Middle Atmosphere Dynamics*; Academic: San Diego, CA, USA, 1987; 489p.
58. Myhre, G.; Alterskjær, K.; Stjern, C.W.; Hodnebrog, Ø.; Marelle, L.; Samset, B.H.; Sillmann, J.; Schaller, N.; Fischer, E.; Schulz, M.; et al. Frequency of extreme precipitation increases extensively with event rareness under global warming. *Sci. Rep.* **2019**, *9*, 16063. [CrossRef] [PubMed]
59. Brown, A.T.; Volk, C.M.; Schoeberl, M.R.; Boone, C.D.; Bernath, P.F. Stratospheric lifetimes of CFC-12, CCl_4, CH_4, CH_3Cl and N_2O from measurements made by the Atmospheric Chemistry Experiment-Fourier transform spectrometer (ACE-FTS). *Atmos. Chem. Phys.* **2013**, *13*, 6921–6950. [CrossRef]
60. Prather, M.J.; Froidevaux, L.; Livesey, N.J. Observed changes in stratospheric circulation: Decreasing lifetime of N_2O, 2005–2021. *Atmos. Chem. Phys. Discuss.* 2022; *in review*. [CrossRef]
61. Ko, M.; Newman, P.; Reimann, S.; Strahan, S. (Eds.) *SPARC: Report on the Lifetimes of Stratospheric Ozone-Depleting Substances, Their Replacements, and Related Species*; SPARC Report No. 6, WCRP-15; SPARC: Zurich, Switzerland, 2013.
62. Randel, W.J.; Wu, F.; Voemel, H.; Nedoluha, G.E.; Forster, P. Decreases in stratospheric water vapor after 2001: Links to changes in the tropical tropopause and the Brewer–Dobson circulation. *J. Geophys. Res. Atmos.* **2006**, *111*, D12312. [CrossRef]
63. Shu, J.C.; Tian, W.S.; Austin, J.; Chipperfield, M.P.; Xie, F.; Wang, W.K. Effects of sea surface temperature and greenhouse gas changes on the transport between the stratosphere and troposphere. *J. Geophys. Res. Atmos.* **2011**, *116*, D02124. [CrossRef]
64. Seviour, W.J.M.; Butchart, N.; Hardiman, S.C. The Brewer–Dobson circulation inferred from ERA-Interim. *Q. J. R. Meteorol. Soc.* **2012**, *138*, 878–888. [CrossRef]
65. Lin, P.; Fu, Q. Changes in various branches of the Brewer–Dobson circulation from an ensemble of chemistry climate models. *J. Geophys. Res. Atmos.* **2013**, *118*, 73–84. [CrossRef]
66. Remsberg, E.E. Methane as a diagnostic tracer of changes in the Brewer–Dobson circulation of the stratosphere. *Atmos. Chem. Phys.* **2015**, *15*, 3739–3754. [CrossRef]
67. Han, Y.Y.; Tian, W.S.; Zhang, J.K.; Hu, D.Z.; Wang, F.Y.; Sang, W.J. A case study of the uncorrelated relationship between tropical tropopause temperature anomalies and stratospheric water vapor anomalies. *J. Trop. Meteorol.* **2018**, *24*, 356–368.
68. Birner, T.; Bönisch, H. Residual circulation trajectories and transit times into the extratropical lowermost stratosphere. *Atmos. Chem. Phys.* **2011**, *11*, 817–827. [CrossRef]
69. Proffitt, M.H.; Margitan, J.J.; Kelly, K.K.; Loewenstein, M.; Podolske, J.R.; Chan, K.R. Ozone loss in the Arctic polar vortex inferred from high-altitude aircraft measurements. *Nature* **1990**, *347*, 31–36. [CrossRef]
70. Liu, Y.; Lu, C.H.; Wang, Y.; Erkki, K. The quasi-biennial and semi-annual oscillation features of tropical O_3, NO_2, and NO_3 revealed by GOMOS satellite observations for 2002–2008. *Chin. Sci. Bull.* **2011**, *56*, 1921–1929. [CrossRef]
71. Ern, M.; Diallo, M.; Preusse, P.; Mlynczak, M.G.; Schwartz, M.J.; Wu, Q.; Riese, M. The semiannual oscillation (SAO) in the tropical middle atmosphere and its gravity wave driving in reanalyses and satellite observations. *Atmos. Chem. Phys.* **2021**, *21*, 13763–13795. [CrossRef]
72. Wang, W.K.; Hong, J.; Shangguan, M.; Wang, H.Y.; Jiang, W.; Zhao, S.Y. Zonally asymmetric influences of the quasi-biennial oscillation on stratospheric ozone. *Atmos. Chem. Phys.* **2022**, *22*, 13695–13711. [CrossRef]
73. Ribera, P.; Peña-Ortiz, C.; Garcia-Herrera, R.; Gallego, D.; Gimeno, L.; Hernández, E. Detection of the secondary meridional circulation associated with the quasi-biennial oscillation. *J. Geophys. Res. Atmos.* **2004**, *109*, D18112. [CrossRef]
74. Garfinkel, I.C.; Shaw, A.T.; Hartmann, L.D.; Waugh, W.D. Does the Holton-Tan Mechanism Explain How the Quasi-Biennial Oscillation Modulates the Arctic Polar Vortex? *J. Atmos. Sci.* **2012**, *69*, 1713–1731. [CrossRef]